Chapter 3

Synthesis and characterization of Mg-Al based LDHs and tailoring of drug release rate for effective cancer treatment

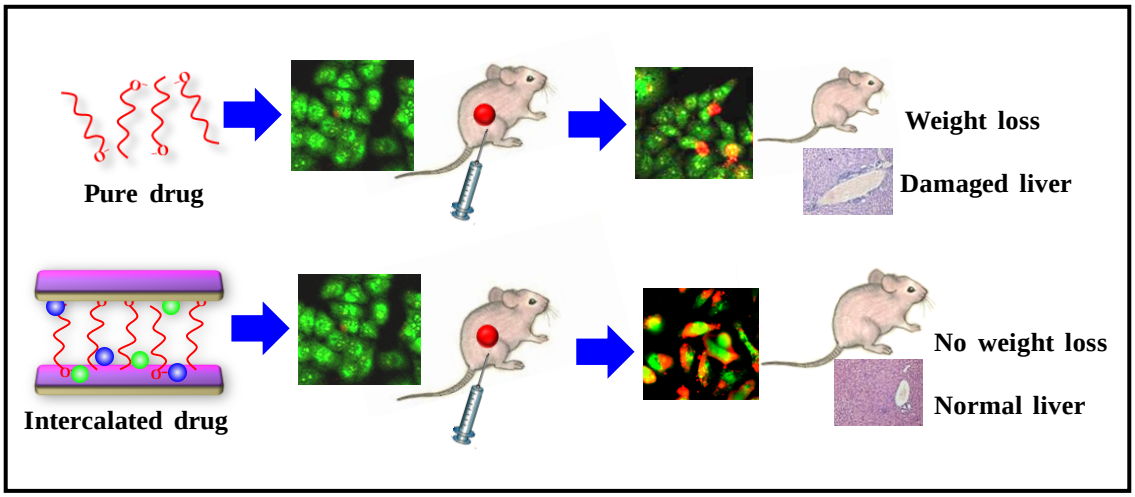

This chapter describes synthesis of a series of Mg-Al based LDH nanocarriers with varying interlayer anions for controlled delivery of anticancer drug. The developed nanocarriers potentially enhance therapeutic efficacy of the drug while reduce its adverse side effects.

3.1 Introduction:

In past few decades, various drug delivery vehicles have been developed to improve the efficiency of chemotherapeutics. Among them, polymer nanoparticles, micelles and lipids (liposomes) are the most widely explored vehicles [Brigger et al., 2002; Yang et al., 2013; Yang et al., 2015 Nicolas et al., 2013; Haley et al., 2008]. Inorganic nanocarriers are emerging as strong competitors in recent years due to their potential advantages, such as enlarged surface area, greater drug loading capacity, improved bioavailability, lower toxic side effects, controlled release of drug and unlike polymer-based carriers they can tolerate most organic solvents [Hanafi-bojd et al., 2015; Yu et al., 2015; Lu et al., 2007 Bhattacharyya et al., 2011; Yu et al. 2008].

Layered double hydroxides (LDHs), a family of anionic clay materials, are considered promising inorganic nanocarriers due to their several attractive features, such as high layer charge density (2-5 mequiv/g), high anion exchange capacity, excellent biocompatibility, low toxicity, pH-controlled release, tunable particle size [Tagaya et al., 1993; Del Hoyo et al., 2007; Goh et al., 2008]. The host layers of LDHs possess net positive charges which are counter balanced by the interlayer anions and those anions are exchangeable with other suitable negatively charged moieties. This anion exchange capability of LDHs can be employed to intercalate negatively charged bioactive molecules such as amino acids [Aisawa et al., 2006], vitamins [Gasser 2009], DNA [Choy et al., 1999], siRNA [Chen et al., 2013] and drugs [Panda et al., 2009**;** Yang et al., 2007] within the LDH interlayer gallery. Thus, LDHs can be used as potential drug carrier and may be used to tune the release of drug from the drug intercalated LDH. Controlled drug delivery systems have the advantages that they potentially reduce the frequency of dose administration and thereby improve patient compliances, drug utilization, minimize fluctuations in plasma and serum drug concentration, and more

importantly reduce the undesired adverse side effects. Again, in fast release systems, therapeutic blood concentration can quickly be achieved especially for those drugs which have very short lives. Raloxifene hydrochloride (RH) is known to be a potent antitumor drug but its poor bioavailability, arising from low solubility in water, restricts its practical uses [Teeter et al., 2002].

This chapter deals the synthesis of a series of LDHs with various interlayer anions by using coprecipitation techniques, and to tune the drug release rate through structural variations of LDHs. A model hydrophobic antitumor drug, raloxifene hydrochloride (RH) has been intercalated into LDHs using anion-exchange technique. The underlying mechanisms of the drug release process have been studied for the series of LDH having different anions as the counter ions. This study reveals the process of controlled release (both fast and/or sustained release) system as required by altering the interlayer anions. Both *in vitro* and *in vivo* drug release characteristics of free drug and drug loaded LDHs has been investigated considering antitumor efficacy and toxicity as the major parameters. A new drug delivery carrier with controlled drug release rate has been developed to address the poor bioavailability of anticancer drugs (RH) and to reduce its undesired side effects.

3.2 Results and Discussion

3.2.1 Synthesis of various Mg-Al based LDHs and intercalation of drug

Three different Mg-Al based LDHs having different interlayer anions e.g., NO_3^{-1}, CO_3^{-2} and PO_4^{-3} were synthesized using coprecipitation method and these LDHs are abbreviated as LN, LC and LP, respectively. The corresponding drugs (RH) intercalated LDHs are abbreviated as LN-R, LC-R and LP-R respectively. The powder X-ray diffraction (XRD) patterns of pristine LDHs, and drug intercalated LDHs are shown in **Figure 3.1**. The patterns recorded for LDHs precursors exhibit typical layered structures

of Mg-Al based LDHs similar to those reported in the literature [Millange et al., 2000; Costa et al., 2008]. The reflections from (003) basal planes represent the thickness of the brucite layer plus the interlayer spacing and are a function of the size and orientation of the interlayer anions [Kong et al., 2010]. The diffraction peaks appeared from (003), (006) and (009) crystal planes, as well as two well separated (110) and (113) peaks, indicate the formation of well-crystallized LDHs crystal in pristine LN and LC [Gu et al., 2008]. However, the degree of crystallinity of pristine LP is somewhat lower than that of LN and LC as the (003), (006) and (009) basal planes are not very sharp, as well as (110) and (113) peaks are not separated. The (003) basal

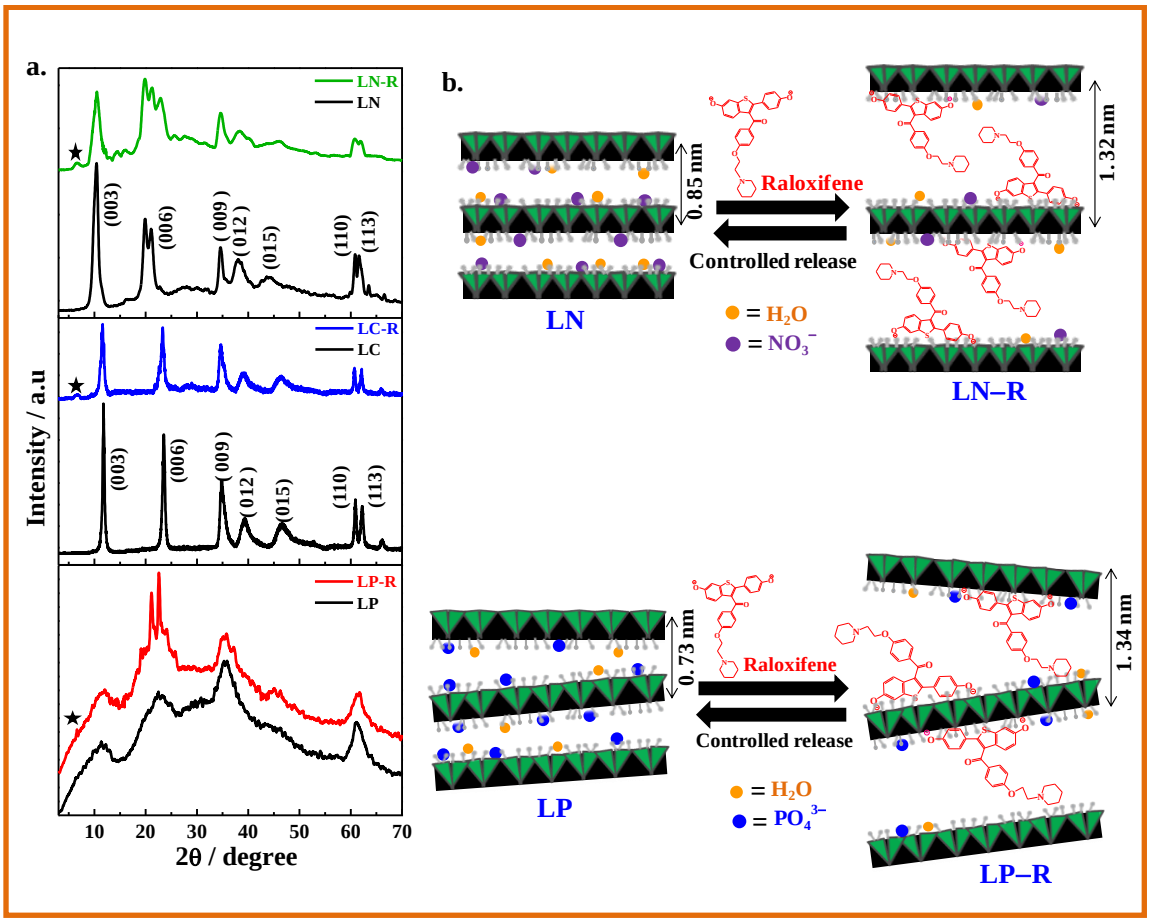

Figure 3.1: (a) XRD patterns of LN, LN–R; LC, LC–R; and LP, LP–R. '∗' marks indicates the new set of basal reflections originates from RH intercalated LDH phases; (b) a schematic drawing of LDH structure before and after drug intercalation in LN and LP.

spacing in LN and LC are 0.85 and 0.75 nm respectively, the same as reported in earlier [Silion et al., 2010; Panda et al., 2009]. The (003) spacing in LP is calculated to be 0.73 nm. After intercalation of drug molecules (RH), (003) and (006) peaks become weak and slightly broad which suggests the lower crystallinity. In addition, a new set of peaks (indicated with the '∗' mark in **Figure 3.1**) appeared at $2\theta \sim 6.67^{o}$, which confirms the intercalation of RH into the interlayer gallery of LDH with the (003) spacing of 1.32 nm for LN–R, and 1.34 nm both for LC–R and LP–R. Thus, an expansion of basal spacing of 0.47, 0.58 and 0.61 nm is found for LN–R, LC–R and LP–R, respectively. Now it is important to understand the relationship between increment of LDH basal height and the charge densities of the interlayer anions. Assuming that all the different three LDHs have similar net positive charge in their brucite-like layers, the number of anions goes down with its increasing charge state and it is believed that the number of interlayer carbonate and phosphate ions is halved and one-third in carbonate-LDH (LC) and phosphate-LDH (LP), respectively, as compared to nitrate-LDH (LN) where interlayer nitrate ions have the single charge state. Hence, the reduced numbers of interlayer anions decrease the gallery height for LC and LP gradually than that of LN. On the other hand, similar basal spacing is obtained in all the drug intercalated LDH samples (1.32 – 1.34 nm) when the extent of drug was kept constant. LN–R and LC–R exhibit ordered crystal structure while in LP–R, the drug molecules are intercalated into the gallery of LP layers with a disordered arrangement and based on the XRD patterns, the nature of intercalation has been shown schematically in **Figure 3.1b** revealing to two different types of nanostructure. Now, it appears that LP-R has more disordered structure or open to the environment for the drugs molecules as compared to the LN-R raising different drug releasing behavior. The XRD profile of pure RH reveals its crystalline nature with the presence of characteristics peaks at 13.46, 14.52, 20.98, 22.62 and 24.1^{o}, which agree

well with the literature [Kushwaha et al., 2013] while the absence of these peaks in intercalated LDHs suggest that the drug molecules are intercalated into the interlayer galleries rather than simple binding to the surface or adsorbed (**Figure 3.2**).

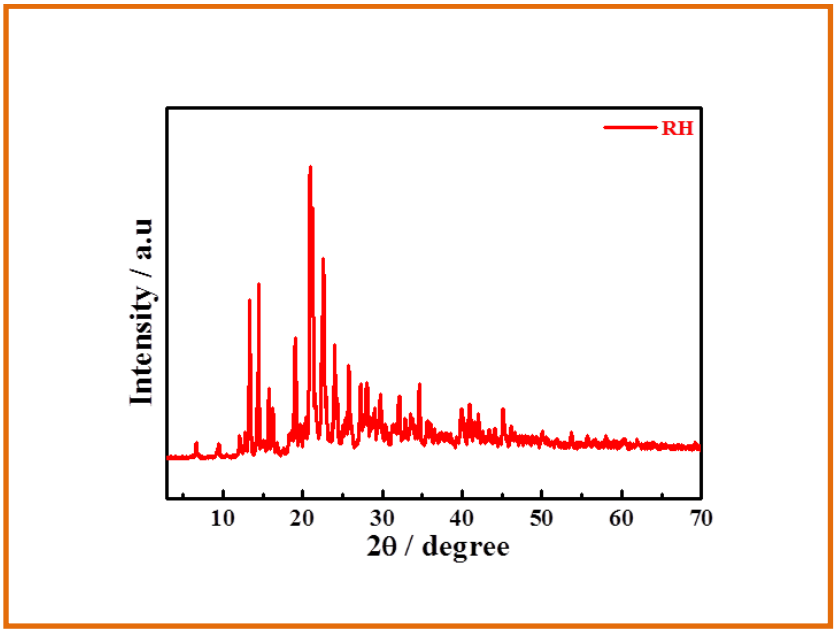

Figure 3.2: XRD patterns of free drug. Pure RH shows its crystalline nature with the characteristics peak at 2θ of 13.46, 14.52, 20.98, 22.62 and 24.1^{o}, which agrees well with the literature.

3.2.2 Structural and morphological changes due to drug intercalation

The shape and sizes of the developed LDH particles have been determined through transmission electron microscopy (TEM). Discrete hexagonal platelet like shaped particles have been observed in pristine LN with the lateral dimension of 84±3 nm while predominantly stacking of platelets and some agglomerated morphology have been observed in the corresponding drug intercalated LDH (LN-R) having the lateral dimension of 94±4 nm (**Figure 3.3a**). After the intercalation of the drug, the stacking force (cohesive force) between the layers and the extensive edge-on hydrogen bonding of the ordered structure make the system more

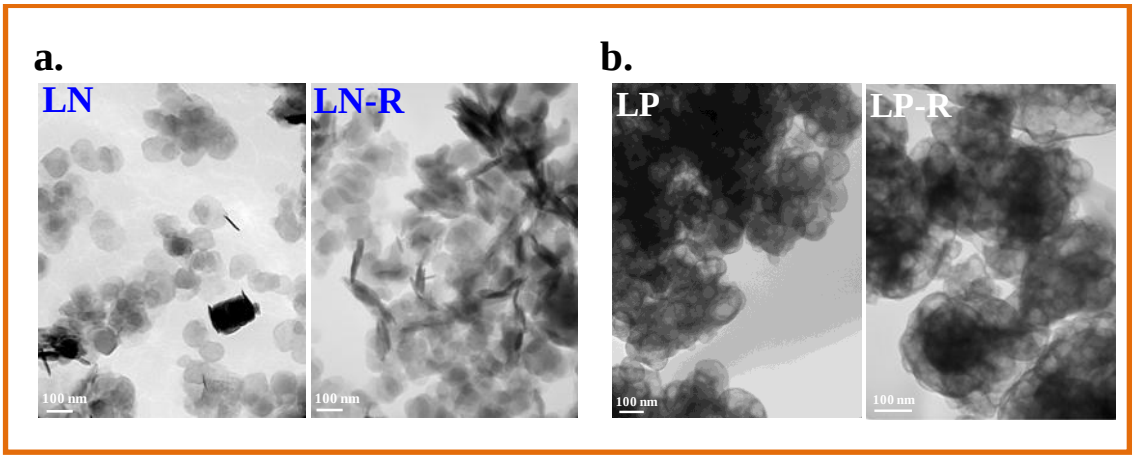

Figure 3.3: Bright field transmission electron micrographs of (a) LN, LN–R and (b) LP, LP–R.

agglomerated [Panda et al., 2009]. The shape and size of these synthesized LDHs are similar to previous published works obtained through bright field TEM images [Zheng et al., 2006]. The morphological characteristics of the other LDHs (LP) and their drug intercalated counterparts (LP–R) are similar to LN system (**Figure 3.3b**). The surface morphology through FESEM of LN and LN–R is shown in **Figure 3.4a**. LN shows a plate-like morphology of dimension 95±2 nm, while after the intercalation of drug in LN–R agglomerates of compact and non-porous granular structure of size 106±3 nm are noticed. **Figure 3.4b** demonstrates the AFM images of the dried suspension indicating relatively larger particle size in LN-R (100 nm) than pristine LN (90 nm). AFM height profiles also indicate the relatively smoother surface in LN-R vis-à-vis pristine LN. However, platelet nature of LDH is obtained which agglomerate extensively after drug intercalation. Dynamic light scattering study reveals that LN, LC and LP have nearly similar particle dimensions of 145±2, 153±2 and 151±3 nm respectively. However, after intercalation of the drug particle sizes become slightly larger as compared to pristine LDHs (**Table 3.1)**.

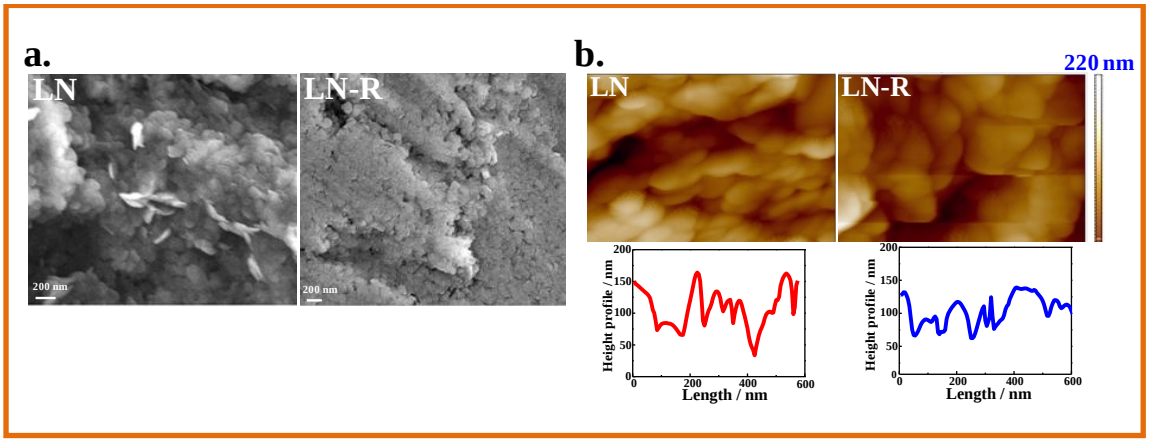

Figure 3.4: FESEM micrographs of (a) LN and LN–R; (b) AFM topographs of LN and LN–R with height profile.

Table 3.1: Particle size, distribution (PDI) and Zeta potential for pristine LDHs and drug intercalated LDHs. Values are presented as mean ± SE (n = 3).

Sample	Particle dimension (nm)	PDI	Zeta potential (mV)
LN	145 ± 2	0.18±0.07	41.3
LN–R	174 ± 5	0.20± 0.08	21.4
LC	153 ± 2	0.17±0.05	42.3
LC–R	178± 4	0.19± 0.06	21.5
LP	151 ±3	0.19±0.07	42.1
LP–R	188±6	0.23±0.09	22.6

Intercalation of the drug molecules (RH) into LDH interlayer gallery is also confirmed by comparing the FTIR spectra for drug intercalated LDHs, in comparison with pristine LDHs and raloxifene hydrochloride **(Figure 3.5)**. The spectrum of pristine LN exhibits the intense broadband around 3445 cm^{-1} associated with the stretching vibration of the hydroxyl groups of LDH host layers and interlayer water molecules **(Figure 3.5a)**. The band appears at ~1630 cm^{-1} is due to bending vibration of water molecules present in the

interlayer gallery. The sharp band at 1384 cm^{-1} is associated with the v_3 stretching vibration of NO_3^- groups. The peak appears at 551 cm^{-1} is assigned to M–O and M–O–H stretching vibrations in the brucite-like host layers of the LDHs. In the lower wavenumber range, the band at 447 cm^{-1} is a characteristic peak of Mg_2Al–LDH [Panda et al., 2009]. In the FTIR spectrum of pure raloxifene, the characteristic peaks at 1643 cm^{-1} (C=O stretching), 1598 cm^{-1} (–C–O–C– stretching), 1466 cm^{-1} (–S–benzothiophene), 1260 cm^{-1} (alkyl–O–phenyl stretching) and 905 cm^{-1} (benzene ring) are observed, which are the same as reported in earlier literature [Kushwaha et al., 2013].

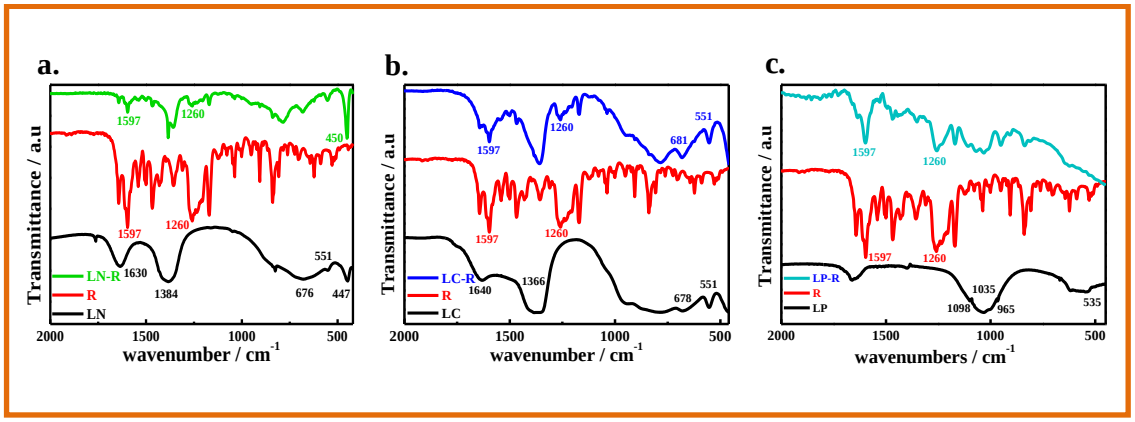

Figure 3.5: FTIR spectra for drug intercalated LDHs, in comparison with pristine LDHs and raloxifene hydrochloride for (a) nitrate based LDH systems, (b) carbonate based LDH systems and (c) phosphate based LDH systems.

After the drug intercalation, LN–R shows diluted (low intense) characteristic peak of nitrate group at 1384 cm^{-1} confirming the exchange of nitrates ions with the raloxifene ions and the other prominent drug peaks. Pristine LC exhibits characteristic peaks of carbonate LDHs at 1640 cm^{-1} (bending vibration of interlayer water molecules), 1366 cm^{-1} (antisymmetric ν_3 vibration of CO_3^{2-}), 678 cm^{-1} (M–O stretching vibration) and 551 cm^{-1} (translational mode of M–OH) [Kapusetti et al., 2012] (**Figure 3.5b**). Similarly, FTIR spectra for LP system shows the characteristic peaks at 1098 cm^{-1} (asymmetric P–

O str.), 1035 cm^{-1} (symmetric P–O str.), 965 cm^{-1} (asymmetric P–OH stretching vibration), and 535 cm^{-1} (asymmetric O–P–O stretching vibration) (**Figure 3.5c**) [Meejoo et al., 2006]. The characteristic peaks for carbonate and phosphate groups become low intense (diluted) in the drug intercalated LC–R and LP–R and appearance of the drug peaks confirms the intercalation of raloxifene ions into the interlayer gallery.

3.2.3 *In vitro* controlled release: tailoring of release rate using different anions

In vitro anticancer drug delivery has been studied with raloxifene intercalated LDHs of varying nanostructure in PBS medium of pH 7.4 to investigate the kinetics of drug release profile through UV-Vis spectroscopy. Drug release patterns for LN–R, LC–R and LP–R with 15 wt.% drug intercalation are shown in **Figure 3.6a**. LP-R exhibits very fast release kinetics; almost 80% drug release occurs in just 1 h and total release accomplishes within 7 h. In contrary, LN–R follows a biphasic elution kinetics, with a relatively slow release rate (~ 65% of the drug released in the first 6 h) followed by a sustained release kinetics (100 % in 42 h from the initial stage). LC–R also follows a similar biphasic release pattern, more than 80% of drug is released at the first 5 h and total release accomplishes around 26 h. It is also observed that the extent of drug intercalation does not affect much the nature of release kinetics with varying drug content (5% and 30% w/w) in LDHs (**Figure 3.6b and Figure 3.6c**). A gradual sustained drug release profile is clearly observed for $PO_4^{3-} \rightarrow CO_3^{2-} \rightarrow NO_3^-$ containing LDHs irrespective of percentage of drug loading. The fast drug release profile in LP-R is anticipated from its disordered pattern of LDH host layers where the intercalated drug is exposed more towards the releasing media while ordered intercalated structure restricts the easy release of drug molecules from LN-R (**Figure 3.6d**).

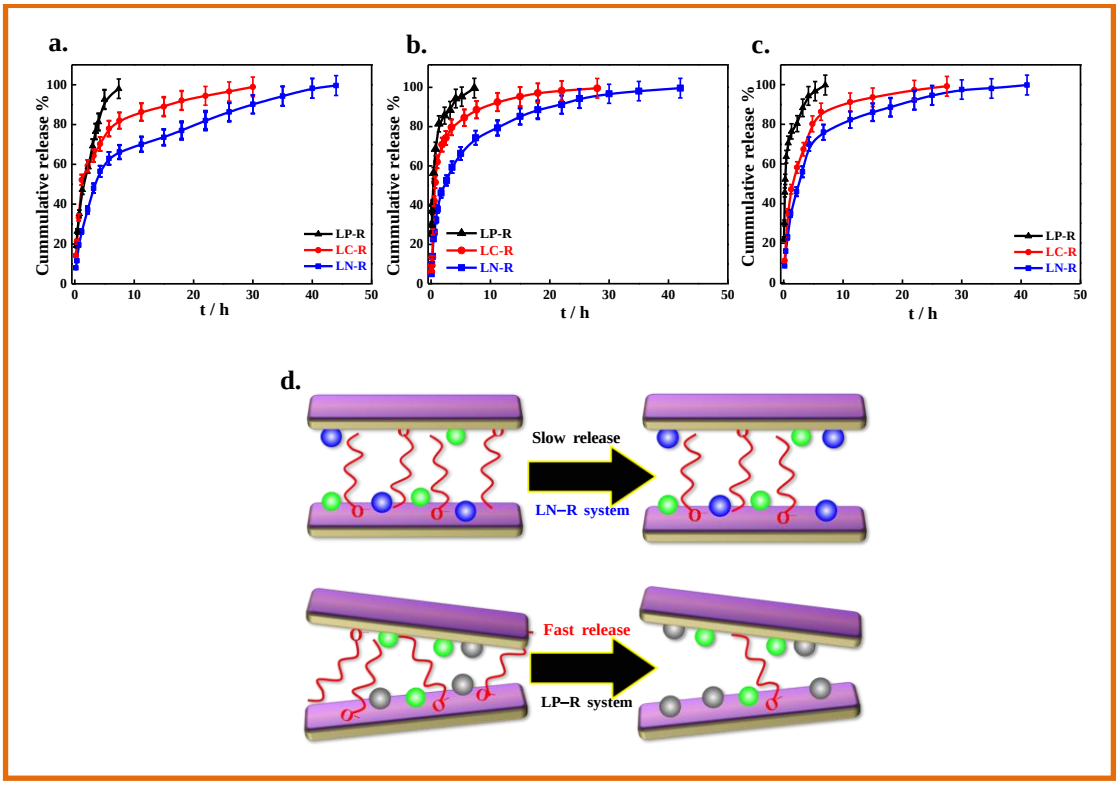

Figure 3.6: *In vitro* drug release profiles for LN–R, LC–R and LP–R with (a) 5% drug intercalation, (b) 15% drug intercalation and (c) 30% drug intercalation. Similar patterns of release profile have been observed suggesting that the extent of drug intercalation does not affect much the nature of release profile. The results presented are mean ± standard deviation (SD) values obtained from three independent experiments. (d) Schematic drawing of drug release behavior from LN-R and LP-R systems.

Further, to investigate the release mechanism of the drug (RH) from the intercalated LDHs, five different kinetic models (zero-order, first-order, modified Freundlich, parabolic diffusion and Elovich model) have been employed. The rate constants and the linear correlation coefficient (r^2) values obtained from the linear fittings of the drug release data are presented in **Table 3.2**. Among these kinetic models, zero- and the first-order models give poor r^2 values ranging from 0.565 to 0.879 and are found not suitable to explain the drug release mechanisms. On the contrary, the the modified Freundlich,

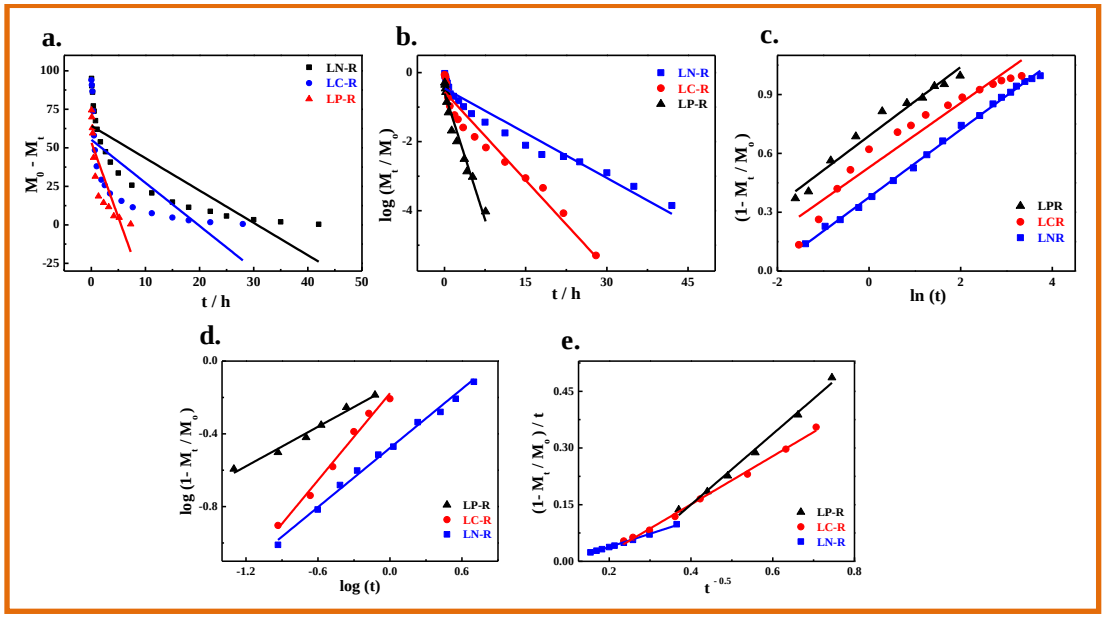

Figure 3.7: Linear fitting of the drug release data to various kinetic models, (a) zero order model, (b) first order model, (c) Elovich model, (d) modified Freundlich model and (e) parabolic diffusion model.

parabolic diffusion model and the Elovich models explain the release profiles more reasonably. Again, to gain more insights of the release mechanism, the whole release profile can be subdivided into two steps: 1) the rapid release stage I (up to 70% cumulative release) followed by, 2) the slow release stage II (70-100% release). It is found that stages I and II are best fitted with the modified Freundlich and parabolic diffusion models, respectively (r^2 ~ 0.98–0.99) (**Figure 3.7**). The modified Freundlich model explains heterogeneous diffusion from the flat surfaces through both diffusion controlled and ion-exchange phenomena and thus is better suitable for initial release while the parabolic diffusion model describes the release of the drug via a diffusion controlled mechanism through intra-particle diffusion or surface diffusion. The Elovich model describes a number of process including bulk and surface diffusion, as well as activation and deactivation of catalytic surfaces [Li et al., 1999; Kodama et al., 2001]. Thus, these mathematical simulation results suggest strongly that the release of the drug

molecules from the LDHs interlayer gallery is a mix-effect including dissolution of nanoparticles

Table 3.2: Rate Constants and Linear Correlation Coefficients (r^2) Obtained by Fitting the RH Release Data from LN–R, LC–R and LP–R.

kinetic models	LN–R			LC–R			LP–R		
	I	II	III	I	II	III	I	II	III
zero-order model									
k_0	11.20		2.13	45.24		2.68	60.2		9.76
r^2	0.847		0.707	0.914		0.527	0.942		0.676
first-order model									
k_1	0.227		0.086	0.740		0.170	1.220		0.492
r^2	0.887		0.923	0.901		0.931	0.911		0.936
parabolic diffusion model									
k_d	0.39	0.349	0.345	0.685	0.627	0.667	1.26	0.966	1.139
r^2	0.925	0.996	0.946	0.955	0.993	0.969	0.961	0.992	0.976
modified Freundlich model									
k_m	0.333	0.525	0.288	0.617	0.669	0.380	0.727	0.779	0.645
r^2	0.991	0.982	0.932	0.987	0.976	0.914	0.981	0.969	0.950
Elovich model									
k_e	0.178	0.155	0.172	0.326	0.108	0.164	0.250	0.110	0.175
r^2	0.991	0.982	0.932	0.987	0.976	0.914	0.981	0.969	0.950

I For 0–70 % release. II For 70–100 % release. III For the whole release process (0–100 %).

and ion-exchange between the intercalated anions in the lamellar host and the phosphate anions in the buffer solution. In stage I, most of the drug molecules from intercalated drug (RH) dissociate from the surface of LDHs and diffuse into the releasing medium via anion exchange, responsible for the fast release, whereas diffusion of the drug molecules from the interlayer gallery of LDH is the rate-controlling step in stage II, that prolongs the release time [Kong et al., 2010; Gu et al., 2008]. As shown in **Table 3.2,** the rate constants (k_d) of the LN–R system is found to be less than that of LC–R, which in turn less as compared to LP–R using parabolic diffusion model. Similar trends of release rate constants (k_d) is also found for modified Freundlich and the Elovich models fittings.

Therefore, these observations clearly suggest that the release of drug molecules from LN–R nanohybrid is more difficult as compared to LC–R, whereas the release kinetics are more sluggish than LP–R. Interactions between drug and LDHs might play a role for the fast or sluggish release which will be uncovered in the next section.

3.2.3 Interactions between drug and LDH

X-ray photoelectron spectroscopy (XPS) is used to unveil the nature of interactions between LDH and drug molecules. A significant amount of shifting in the XPS Al 2p peak has been observed to higher binding energy side in LN-R nanohybrid as compared to pristine LN (73.65 to 74.2 eV, *i.e.*, Δ BE = 0.55 eV) against the meager increment observed in LP-R nanohybrid vis-à-vis pristine LP (74.68 to 74.77 eV, *i.e.*, Δ BE = 0.09 eV) strongly suggest the greater interaction between the drug molecules and LDH host layers in LN-R as compared to LP-R (**Figure 3.8a**). The shifting in binding energy for LC-R with respect to pristine LC is observed to be moderate (73.86 to 74.08 eV *i.e.*, Δ BE = 0.22 eV). Similar patterns of results are also noticed for Mg 2p XPS peak and the differences in binding energies are 0.01, 0.15 and 0.39 eV for LP-R, LC-R and LN-R systems, respectively, as compared to their respective pristine LDHs **(Figure 3.8b).** Hence, these XPS results clearly suggest that the drug molecules strongly interact with LN while the extent of interactions goes down in LC and LP gradually [Dou et al., 2012; Shimamura et al., 2012; Podsiadlo et al., 2007].

Figure 3.8c demonstrates the comparative solid state UV-Vis spectra of pure LDHs, pristine drug and drug intercalated all the three LDH nanohybrids. Pure drug exhibits the characteristic peaks at 225, 266 and 364 nm while pristine LN exhibits strong absorption band at 221 and 293 nm. However, LN–R shows absorption band at 226, 295 and 392 nm indicating strong red shift of the peaks especially for the 266 and 364 nm bands where Δλ

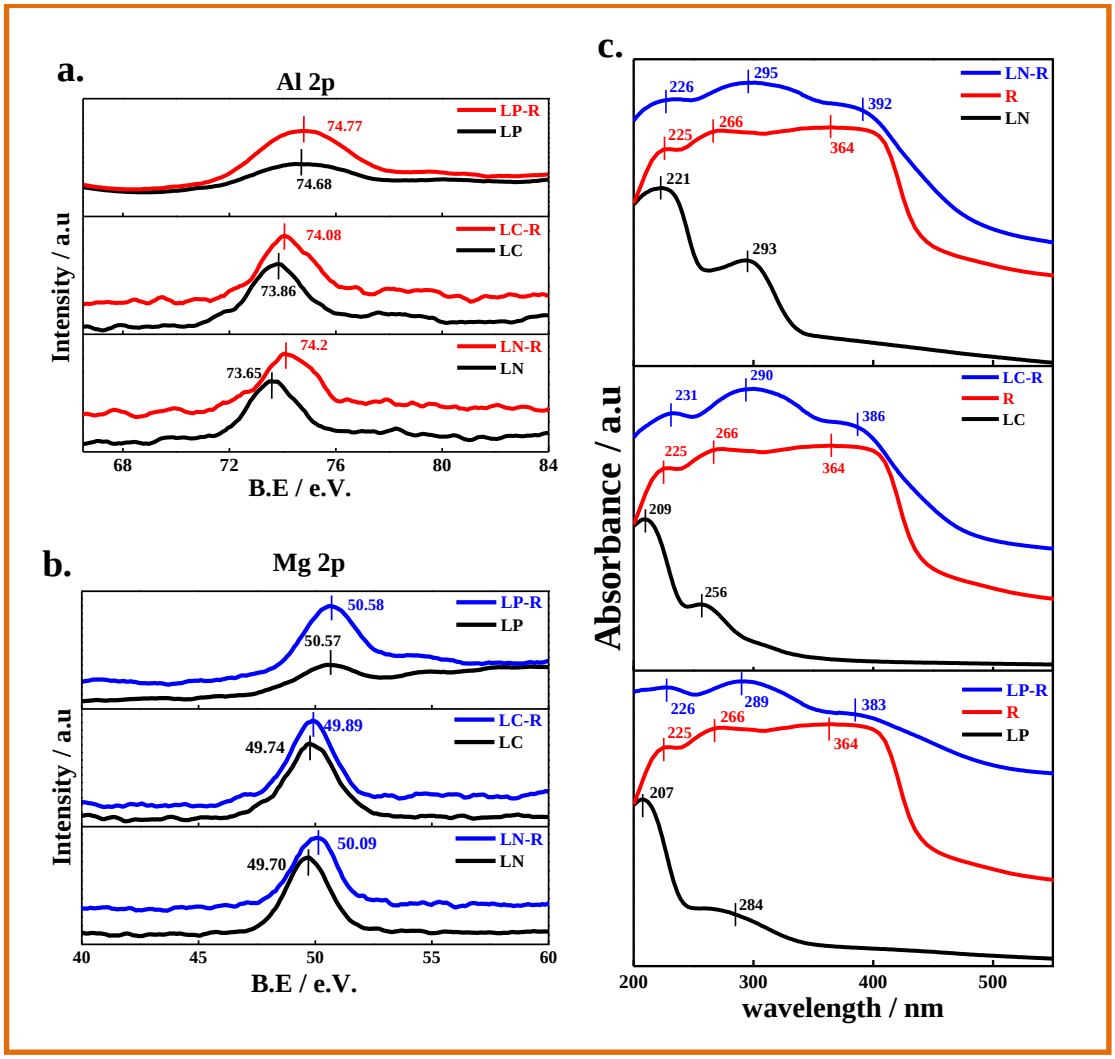

Figure 3.8: (a) Al 2p and (b) Mg 2p XPS spectra for pristine LDHs and drug intercalated LDHs. The vertical lines indicate the peak position/binding energy; (c) comparison of solid-state UV−vis spectra of various pristine LDHs, pure drug (RH), drug intercalated LDHs.

is 28 nm against the relatively lower shifting (Δλ ~ 19 nm) noticed for LP-R. Again, the absorption peak of RH appears at 286 nm in LC-R with a red shifting of ~22 nm. This red shift of the absorption peaks is an indicator of amount interaction between the drug and LDHs host layer. The relatively greater shifting in LN-R suggests stronger interactions as compared to LC-R and LP-R. Hence, both the XPS and UV-Vis investigations clearly indicate that the order of interactions between the drug molecules and LDHs is LN-R > LC-R > LP-R and based on this order of interactions, one can easily

explain the fast drug release behaviour using LP-R and sustained release profile with LN-R. It is now important to understand the reason behind the variation of amount of interactions in all three cases where the drug molecules and basic constituents of LDHs are same with the changes in exchangeable interlayer anions. The charge densities of the interlayer anions in this study alter from nitrate to carbonate to phosphate and the electrostatic interaction between the triply charged phosphate ions and LDH host layers is the highest which intern causes the lowest interaction between drug and host layers in LP-R nanohybrid. In contrary, singly charged nitrate anion is attracted by the LDH host layer in a relatively weak force and then drug molecules interact with the rest of the layer in greater way leading to the above order (LN-R > LC-R > LP-R) of interactions between the drug molecules and LDHs.

3.2.4 Thermal properties: Interactions and stability

Differential scanning calorimetry (DSC) analysis was performed to understand the interaction between drug molecules and different types of LDH as host layers. The depression of melting temperature of the drug along with heat of fusion is considered to be the extent of interaction between the components. **Figure 3.9a** shows the DSC thermograms of pristine drug and all three drug intercalated LDH nanohybrids (LN–R, LC–R and LP–R). The pristine drug exhibits a well defined endothermic peak (melting temperature, T_m) at 264 ^oC which indicates its crystalline nature. The melting temperature of the drug in different drug intercalated LDHs reduces as compared to pure drug and the T_m gradually decreases in the order of LP–R (232.3 ^oC), LC–R(211.7 ^oC) and LN–R (194.2 ^oC) demonstrating significant reduction of T_m in intercalated systems compared to the pure drug (264 ^oC). Again, the heat of fusion, ΔH associated with the melting of drug gradually reduces to 75 and 64 $J.g^{-1}$ for LP-R and LN-R, respectively,

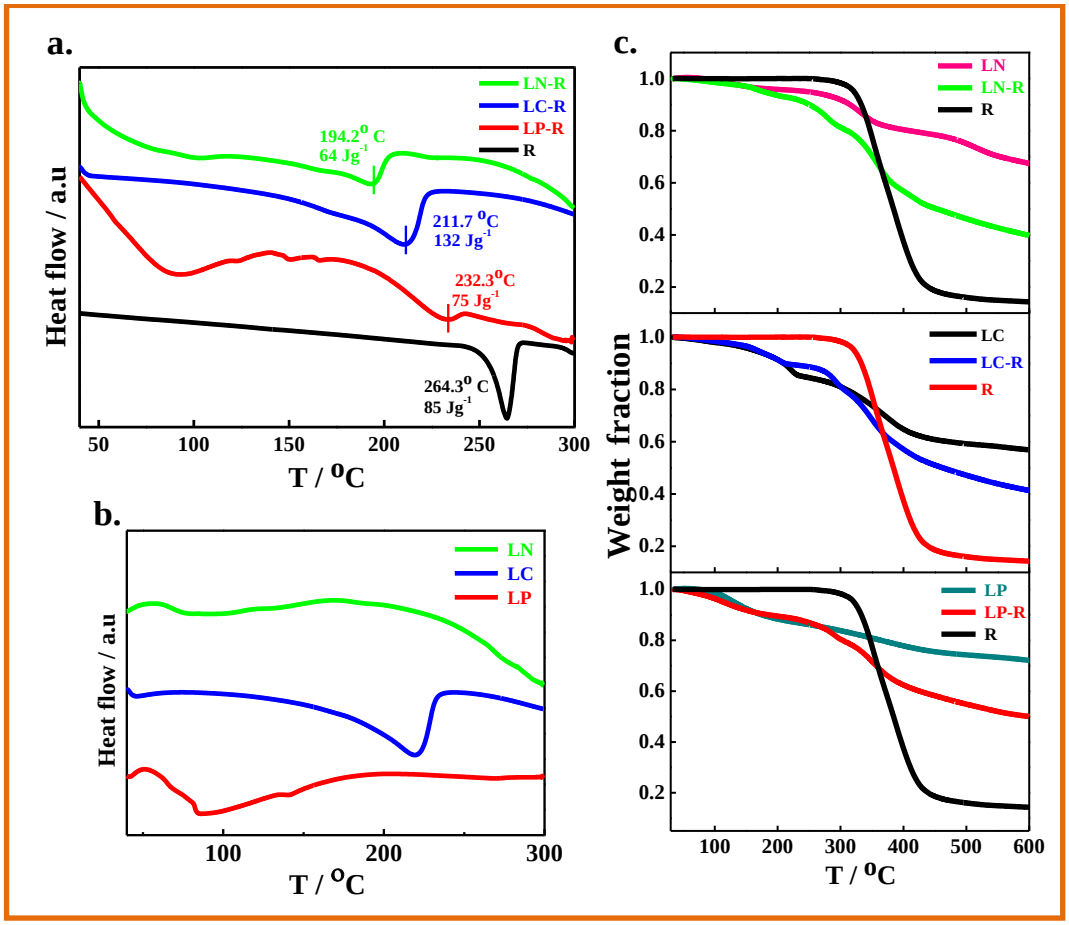

Figure 3.9: DSC thermograms for (a) free drugs and drug intercalated LDHs, (b) pristine LN, LC and LP systems; in pure LC degradation of carbonate species at the region 210-235 ^{o}C is occurred. (c) TGA thermograms NO3–LDH, CO3–LDH and PO4–LDH systems.

from its original value of 85 J.g^{-1} for the pure drug. Therefore it is obvious that the extent of interaction decreases in the order of LN-R > LC- R > LP-R as observed from the relative reduction in T_m and ΔH. This is to mention that ΔH value of LC–R system is relatively large (132 J.g^{-1}) as compared to LN-R or LP-R nanohybrids and is understood from the fact that simultaneous degradation of carbonate species from LC in addition to the regular melting of drug as evident from the DSC thermogram of pristine LC (**Figure 3.9b**). In contrary, no considerable degradation is observed either in pristine LN or LP LDHs.

Therefore, in accordance with XPS and UV studies, DSC analysis also confirms the relative interactions between drug molecule and LDHs host layer is in the order of LN-R > LC-R > LP-R.

The comparative weight loss characteristics of pristine LDHs, drug intercalated LDH and pure drug under heat program in nitrogen atmosphere has been demonstrated in **Figure 3.9c**. In TGA analysis, three stages weight loss behaviour are clearly noticed for pristine LN and LP. The first step corresponds to the weight loss of adsorbed water molecules along with hydrogen bonded and it happens in the temperature range of 100 ^{o}C with ~ 4% weight loss [Wang et al., 2012]. The second stage of weight loss takes place between 170 - 380 ^{o}C and is associated mainly with the dehydroxylation of LDH host layers with ~16% weight loss. The third stage of weight loss occurs in the temperature range of 380 to 540 ^{o}C which accounts for ~12% weight loss resulting from the elimination of interlayer NO_3^- ions. The final decomposition products are MgO and Al_2O_3 at a temperature of 650 ^{o}C with ~ 32% total weight loss [Bontchev et al., 2003]. However, pure drug follows single stage degradation in the temperature region of 280–450 ^{o}C while the drug intercalated LN-R shows 5% weight loss at 177 ^{o}C. On contrary, 5 wt.% loss takes place in LP-R at a temperature of ~114 ^{o}C indicating relatively lower thermal stability of LP-R as compared to LN-R. The greater thermal stability of LN-R is attributed to the ordered stacking patterns where drug molecules are shielded by the LDH host layers while the drug molecules are relatively more exposed in the disordered structure of LP-R resulting lower degradation temperature. The details of degradation characteristics of all the systems have been presented in the **Table 3.3**.

Table 3.3: Degradation temperature of various systems measured from the 5% wt. loss temperature.

System	$T_{deg.}$ / °C
LN	**247**
LN-R	**177**
LC	**163**
LC-R	**167**
LP	**131**
LP-R	**114**
RH	**321**

3.2.3 Biocompatibility and *in vitro* anti-tumor efficacy:

For any drug delivery vehicle, it is necessary that the material (pure LDHs) should be biocompatible itself while the drug intercalated LDHs must have the ability to kill the affected cells depending on the release kinetics of the drug. The *in vitro* cancer suppression performance of pure drug (RH) and RH intercalated LDHs (20 µg/ml) have been evaluated against HeLa cells. The IC50 (half maximal inhibitory concentration) is a quantitative measure of effectiveness of a particular drug against a particular cell line. The IC50 value of the pure drug (RH) against HeLa cells was measured to be 0.79 nM. Cell viability of various materials was determined through MTT assay. As shown in **Figure 3.10a**, the biocompatibility of pure LDHs has been tested with growing number of cells with time suggesting good biocompatibility of the LDHs. On contrary, the percentage cell viability is found to be decreased with time for pure drug and drug intercalated LDHs (**Figure 3.10b**). At the end of day 3, compared with 88±3% cell viability for free RH, a cell viability of 49±2%, 55±3% and 64±3% for LP–R, LC–R and LN–R are observed. Therefore, the drug intercalated LDHs have higher cancer killing

efficiency as compared to the pure drug and instead indicate that LDH can be used as a potential anticancer drug delivery vehicle.

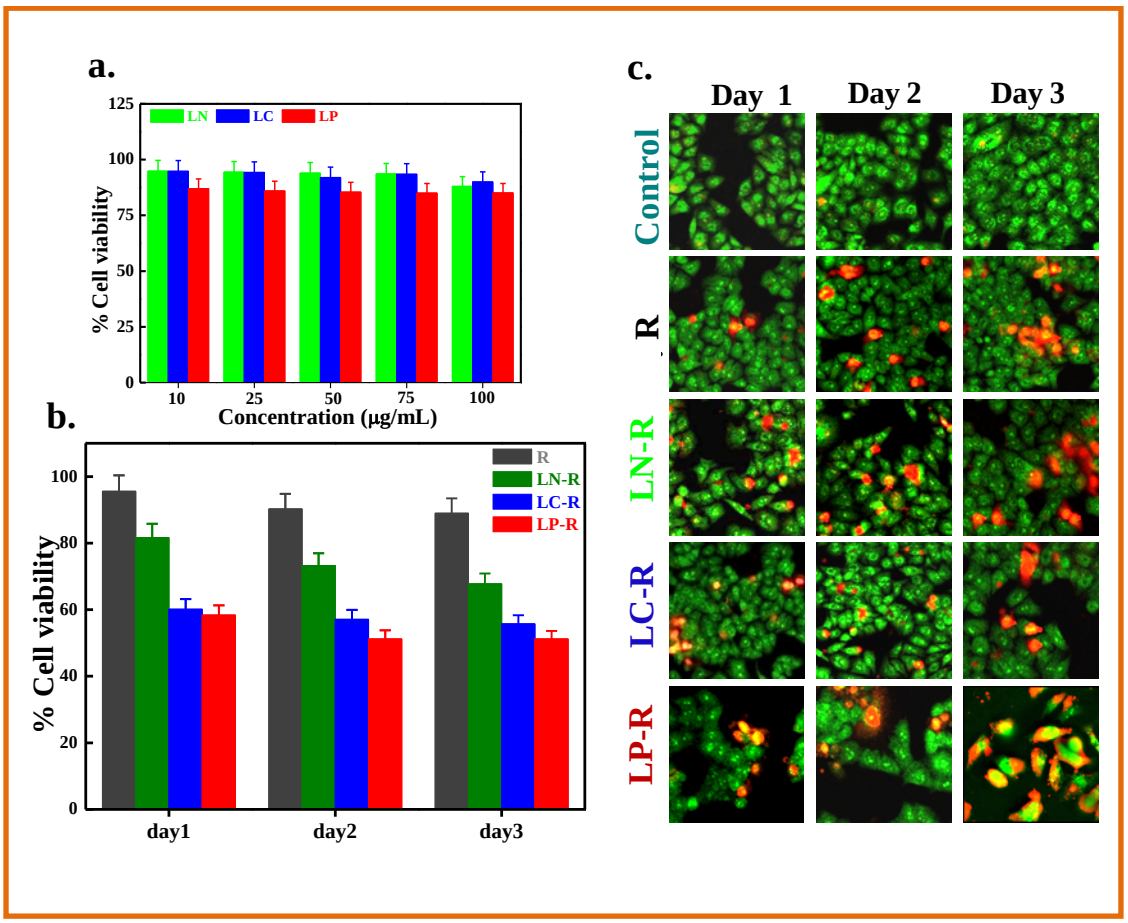

Figure 3.10: (a) Relative cell viability of HeLa cells after incubation of pure nitrate, carbonate and phosphate LDHs (LN, LC and LP respectively) having different concentration, (b) *In vitro* cytotoxicity of free drug and drug intercalated LDHs against HeLa cells with different time intervals; The results presented are mean ± standard deviation (SD) values obtained from three independent experiments, and (c) fluorescent images of AO/EB staining of control, free drug, and drug intercalated LDHs.

Cell membranes are negatively charged in nature and it controls the movements of substances in and out of the cells. When a negatively charged drug molecule approaches towards a cell, it is repelled by the negative charge of the cell membrane resulting poor bioavailibilty of pure drug [Xu et al., 2006; Choy et al., 2001]. Hence, pure RH exhibits a

low cytotoxicity profile against HeLa cells. However, the drug intercalated LDH possesses net positive surface charge as evident from the zeta potential measurements (21–23 mV) **(Table 3.1).** Hence, the drug intercalated LDHs can approach easily and adhere to cell membrane through electrostatic interactions and, thereby, enhances the bioavailability of drug [Choy et al., 2000]. Therefore, a larger number of drug molecules/drug intercalated LDH molecules can pass through the cell membrane in case of drug intercalated LDH systems and, thereby, exhibiting a higher killing efficacy against HeLa cells as compared to pure drug arising from its poor bioavailability. Again, the order of percentage cell viability decreases as LN-R > LC-R > LP-R, which follows the relative rate of drug release from the drug intercalated LDHs.

Furthermore, the relative value of cell viability of different samples is also studied through fluorescence imaging of the HeLa cell after staining with acridine orange and ethidium bromide. The health of the treated cells was monitored as a function of time (after 1 day, 2 day and 3 day of incubation) at a fixed concentration of 20 μg/mL. Based on the permeability of cell membrane, acridine orange and ehidium bromide can distinguish normal cells from apoptotic cells. While acridine orange exhibits green fluorescence, ethidium bromide exhibits red fluorescence when bound to DNA. Usually, dead cells are permeable to both the acridine orange and ethidium bromide showing red fluoresce while the live cells permeate only acridine orange exhibiting green fluoresce [Zhao et al., 2009; Xiang et al., 2011]. **Figure 3.10c** demonstrates a large number of cell deaths in LP-R treated group at different time (yellow to red colored cells depending on early or late apoptosis) while number density of viable cells is more in LN-R treated cells where less amount of drug is being released for a particular time frame which kills less number of cells. In the control system, in absence of any drug, the cell health is perfect as indicated by the green cells only. The number density of viable cells is the highest in case

pure drug as compared to the drug intercalated LDHs. Therefore, the cell viability and morphology studies strongly suggest the better cancer suppression efficiency by the drug intercalated LDH vis-à-vis pure drug.

3.2.4 *In vivo* anti-tumor efficacy and histopathological evidences

The antitumor efficacy of drug intercalated LDHs, LP–R, pure RH and pristine LDHs has been investigated in Balb/c mice after creating similar size (~50 mm^3) of syngenic 4T1 tumor in them. The mice were observed daily for clinical symptoms, and the tumor

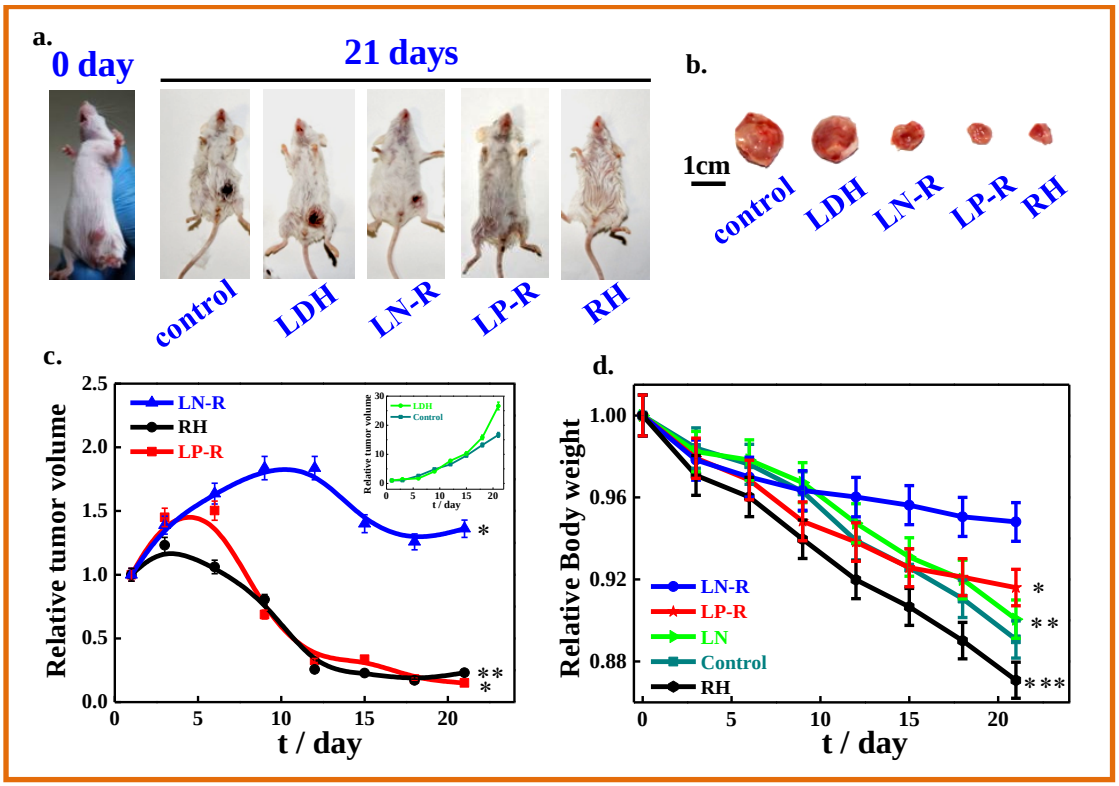

Figure 3.11: *In vivo* tumor suppression performances and systemic toxicity of pure RH and drug intercalated LDHs in comparison to control. (a) Photographs of the mice of different experimental groups at 0 day and at 21 days, (b) excised solid tumors at the 22nd day, (c) relative changes in tumor volume of pure drug and drug intercalated LDHs with time, inset figure shows relative changes in tumor volume of pristine LN and control (PBS) treated groups, and (d) changes in body weight of the animals of the different treatment groups with time, where, $*P < 0.05$, $**P < 0.01$, $***P < 0.001$.

volume and body weight were monitored routinely throughout the experiment. **Figure 3.11a** exhibits the original tumor size (0 day) and the changes in their shape and size after 21 days of post treatment with various samples. Excised tumor volume has been shown in **Figure 3.11b** revealing reduced size in the mice treated with pure drug and drug intercalated LDHs while aggravated size was observed in mice treated with pure LDH and control (treated with PBS). Pure RH and RH intercalated LDHs treated group result in a lowering of tumor volume as compared to control system (PBS or LDH NPs; inset figure of **Fig. 3.11c**) clearly suggests the tumor suppression efficacy of the drug released in vivo for reducing the tumor size (**Figure 3.11c**)**.** The downward tendency of the relative tumor volume of LN-R system has started late as compared to LP-R system basically due to slow drug release behavior in LN-R system. However, LP–R treated group exhibits the best tumor suppression effect due to the smallest tumor volume during the treatment which is attributed to the faster release of RH from the LP–R nanohybrid.

The changes in body weight index are the general symptoms for understanding the activity of the potentially toxic chemicals [Ailey et al., 1999]. To evaluate the undesired adverse effects of different therapy treatments, body weights changes of the tumor-bearing mice have been monitored after the administrations (**Figure 3.11d**). It is found that, body weight of the mice administered with pure drug decreases steeply as compared to the drug intercalated LDHs administered groups presumably due to the serious side effect of pure drug. Moreover, amongst the drug intercalated LDHs, body weight of mice administered with LN–R is higher as compared to the LP–R administered group, although the relative tumor sizes of LP–R administered group are smaller than those of LN–R treated group. Hence, the body organs appear to be healthier in LN-R administered mice even though the healing rate is bit slower as against the faster healing rate in LP-R administered mice which cause damage to other organs, as observed from

greater loss of body weights. Histopathological index is a measure of cell health of the body organs when the animal is administered with therapeutic agents for a definite period of time. The mice were sacrificed on the 21th day of post treatment and the tumors and

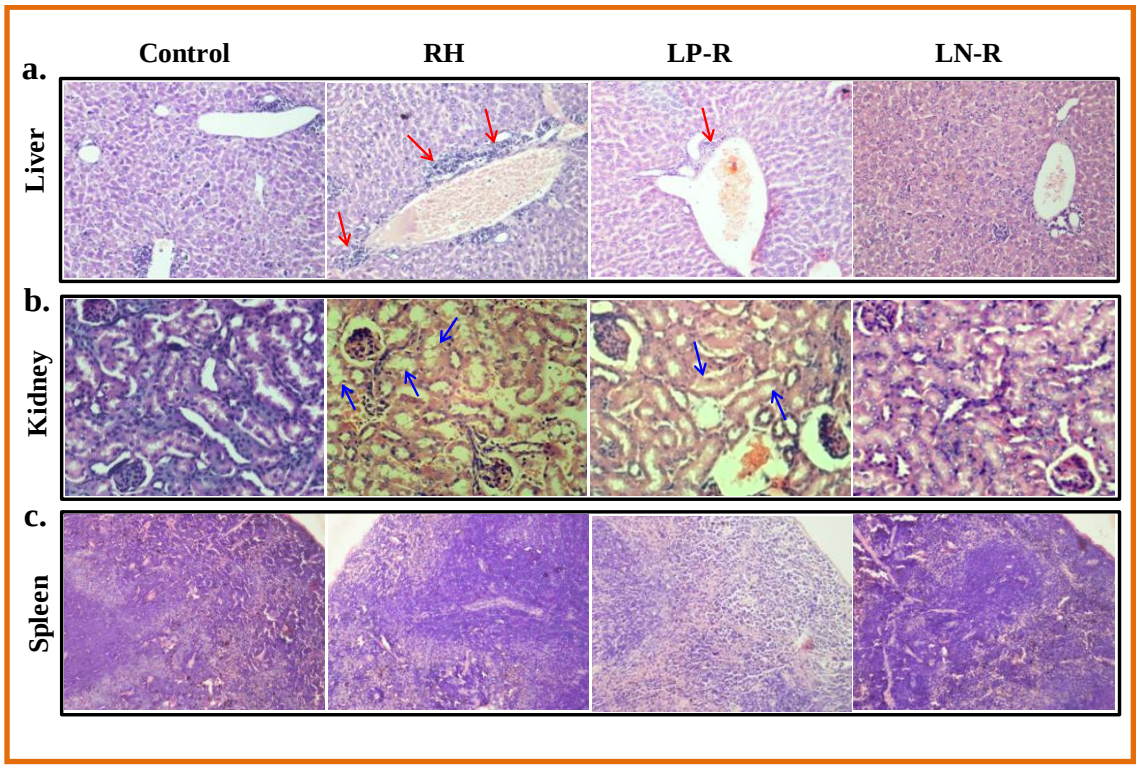

Figure 3.12: Histopathological analysis of (a) liver (b) kidney and (c) spleen of tumor bearing Balb/c mice treated with control (saline), pure RH, LN-R and LP-R (all tissues: 200×). The investigation reveals that the free drug administered mice resulting in bile ductular proliferation and congested portal vein in portal triad (shown by red arrows). Mice administered LP-R shows dilated venous radical withmild congestion (red arrows).Mice treated with pure drug exhibits cloudy degeneration of the tubular epithelial cells in the kidney (shown by blue arrows). A slight damage of tubular cells is also noticed for mice treated with LP-R (blue arrows). However, other organs of mice administered saline and drug intercalated LDH nanoparticles shows no obvious toxicity.

the main organs were excised for tumor volume and histological analysis wherever applicable. Further, hematoxylin and eosin (H&E) stained sections of the liver, kidney and spleen have thoroughly been analyzed to confirm any potential toxicity of pure drug

and drug intercalated LDHs **(Figure 3.12)**. Microphotograph of liver tissues of the mice administered with saline (control) exhibits normal architectural hepatocytes, which are large in size, hexagonal in shape with more or less centrally located one or more nuclei with homogenous cytoplasm. However, the liver of mice administered with pure drug exhibits bile ductular proliferated portal triad, congested portal vein (indicated by arrows) and a loss of normal architecture of the hepatocytes is also observed. Again, mice administered with LP–R exhibits dilated venous radical with mild congestion. In contrast, no obvious liver toxicity of the mice administered with LN–R is noticed. Furthermore, a cloudy degeneration of the tubular epithelial cells in the kidney cells is observed for those mice administered with pure drug. A slight damaged tubular cell is also noticed for mice administered with LP–R system. However, no significant kidney toxicity of the mice administered with LN–R is observed. This is to mention that the mice treated with saline (control) also show normal architecture of kidney. No obvious histopathological abnormalities or lesions are noticed in spleen. This is worth mentioning that pristine LDHs have no toxic side effects as demonstrated by clinical chemistry and histopathology [Kwak et al., 2004] and the side effect in liver and kidney is caused by the released drug either from the pure drug or drug intercalated LP-R. It is now clear that the free drug exposed to blood stream directly or drug intercalated LP (LP-R), which release the drug very fast, engenders strong undesired side effect specially on liver and kidney tissues although the rate of tumor healing are moderately fast in both the cases. On the other hand, LN-R treated group has no adverse side effect but heal the tumor in relatively slow rate proving a much better drug release carrier for cancer treatment.

3.2.5 Pharmacokinetics characteristics of RH intercalated LDHs

The pharmacokinetic properties of pure RH and one representative RH intercalated LDH (LN–R) were evaluted in male Sprague–Dawley rats after intraperitoneal administration

(30 mg drug / Kg body weight and equivalent amount in drug intercalated LDHs). The various pharmacokinetic parameters are summarized in **Table 3.4**. The mean clearance half-life ($t_{1/2}$) are measured to be significantly higher for LN-R treated rats (25 h) as compared to the free drug treated rats (18 h).The mean plasma AUC_{0-72} in rats treated with pure drug and LN–R was calculated to be 644±32 and 694±36 h ng mL^{-1} respectively. The maximum plasma concentration (C_{max}) values for pure drug and LN–R

Table 3.4: Pharmacokinetic parameters of RH after administration of free RH and RH intercalated LDHs to male SD rats with dose equivalent to 30 mg of RH / kg of body weight.

Parameter	Pure RH	LN–R
$t_{1/2}$ (h)	18	25
C_{max}(ng mL^{-1})	45± 6	71±11
T_{max} (h)	3±0.25	3.7±0.11
AUC_{0-72} (h × ng mL^{-1})	644±32	694±36
Bioavailability (%)	2.9±0.5	3.3±0.4

treated rats are 45± 6 and 71 ± 11 ng/mL respectively. The time to reach maximum plasma concentration (T_{max}) for pure drug and LN–R treated groups are 3.0 and 3.7 h respectively. *In vivo* bioavailability of RH intercalated LDH (LN–R) is found to be higher compared to pure RH (i.e., 3.3±0.4 and 2.9± 0.5 % respectively). These *in vivo* pharmacokinetic investigations therefore clearly illustrate that LN–R has improved pharmacokinetics profile than the original pure RH.

3.2.6 *Biochemical parameters: Effect of released drug*

Biochemical properties provide the data base for most examinations and may have specificity for an organ or pathological process. Individual biochemical properties can be employed for therapeutic drug testing. Biochemical parameters of the mice administered with various samples are summarized in the **Table 3.5**. The lowest hemoglobin concentration (11.4 mg/dL) has been found in pure drug treated group. On the other hand, the highest hemoglobin concentration (12.6 mg/dL) and the best blood parameters have been monitored in pristine LN and LN−R administered mice groups. The hemoglobin concentration in the LP−R administered and control groups have almost the similar values (12.3 mg/dL). Liver function test is evaluated by measuring of levels of liver

Table 3.5: Changes of biochemical parameters in the serum of mice induced by pristine LDH, free drug and drug intercalated LDHs.

Groups	**AST (U/L)**	**ALT (U/L)**	**BUN (mg/dL)**	**Hgb (mg/dL)**	**WBC (K/µl)**	**PLT (K/µl)**
Control	118±9.1	38±2.1	56±2.1	12.4±0.3	2.8±0.2	845±31
LN	121±7.4	37±1.9	58±1.9	12.6±0.5	2.8±0.15	832±27
LN−R	121±5.9	38±1.2	60±4.9	12.6±0.8	2.6±0.1	819±21
LP−R	118±4.4	37±2.9	55±3.4	12.3±0.8	2.0±0.5	841±20
RH	116±4.9	39±2.9	63±4.8	11.4 ±0.8	2.6±2.1	833±16

enzymes viz. AST and ALT. The ratio ALT/ AST is a more sensitive indicator for hepatic injury [Wang et al., 2006]. The physiological values of AST and ALT activity in serum for normal mice are generally ~128 and ~32 U/L, respectively [Wang et al., 2012]. An increase in the activities of AST and ALT level in plasma is assigned mainly to the leakage of these enzymes from the liver cytosol into the blood stream which provides an

indication of the hepatotoxic effect [El-demerdash et al., 1998]. The decrease in the liver AST and ALT levels may be due to liver disturbance and dysfunction in the synthesis of these enzymes. ALT/ AST ratio has increased (0.336) in the mice treated with pure drugs while decreases for LP–R, LN–R and LN (~0.305) in comparison to the control (0.322). These results therefore suggest that pure RH induces hepatotoxicity in mice by repeated administration. Hence, it is concluded that the hepatotoxic effect of the free drug can be diminished significantly by intercalating the drug into LDH host layers. The renal function test has also been evaluated by measuring the BUN levels. An elevation of this biomarker activity has been noticed in the mice treated with pure drug (63±4.8 mg/dL) indicating kidney dysfunction. However, BUN levels are observed to be nearly equal for LN, LN–R, LP–R and control (56 – 60 mg/dL). There are no considerable differences in plasma WBC and PLT counts are noticed of all the experimental mice. The biochemical parameters therefore clearly suggest that the toxicity appears in the blood of mice when administered with pure drug while the toxicity markedly diminishes after using drug intercalated inside LDHs confirming LDH as a efficient drug delivery vehicle which releases drug in a controlled manner for the healing of tumor in animal model. This is worthy to mention that the damaged liver/kidney actually increase the activity of ALT/BUN in blood sample of the mice administered with pure drug or LP-R while sustained release of drug from LN-R system does not damage any organ and that is why we observed normal levels of biochemical parameters.

3.3 Conclusion:

Three different Mg-Al based layered double hydroxides (LDHs) nanocarriers have been developed with varying exchangeable interlayer anions ($NO_3^-, CO_3^{2-} and\ PO_4^{3-}$) following the intercalation of a model anticancer drug. Controlled drug delivery has been obtained with very fast rate with phosphate based LDH-drug system (LP-R) while

sustained delivery is obtained using nitrate based LDH (LN-R). *In vitro* anticancer investigation reveals that drug intercalated LDHs efficiently inhibit the growth of HeLa cells as compared to free drug. LP–R shows better tumor suppression efficiency while body weight loss index suggests the damage of organs. In contrast, LN-R exhibits slight slow healing of tumor while it shows minimum body weight. Histopathological analysis of different organs strongly suggests damaged liver cell of mice treated with fast release vehicle (pure drug and LP-R) while no damage occurs in mice liver cell treated with LN-R. Furthermore, analyses of biochemical parameters also reveal that drug intercalated LDH systems have less toxic effects than that of pure drug. Hence, side effects as measured from body weight measurements, histological assessment and analysis of biochemical parameters indicate that drug intercalated LDHs, especially slow releasing system, are safer materials as compared to pure anticancer drug.